

Photoluminescence of Erbium-Doped Silicon: Temperature Dependence

C.A.J. Ammerlaan¹, D.T.X. Thao^{1,2}, T. Gregorkiewicz¹, B.A. Andreev³
and Z.F. Krasil'nik³

¹ Van der Waals-Zeeman Institute, University of Amsterdam,
Valckenierstraat 65, NL-1018 XE Amsterdam, The Netherlands

² International Training Institute for Materials Science, ITIMS Building, Dai hoc Bach Khoa Hanoi,
1 Dai Co Viet Road, Hanoi, Vietnam

³ Institute for Physics of Microstructures, Russian Academy of Sciences,
GSP-105, Nizhny Novgorod, RU-603600 Russia

Keywords: Silicon, Erbium, Photoluminescence

Abstract

The temperature dependence of the photoluminescence intensity of erbium-doped silicon was measured experimentally and modeled theoretically. Measurements were made on float-zoned and Czochralski-grown silicon samples which were doped with erbium by ion implantation and on MBE-grown material. Results are discussed on the basis of a physical model in which following the formation of free electrons and holes by the exciting laser beam, the energy is transferred via the formation of free excitons and the binding of the excitons to erbium ions to the 4f electrons of the erbium ions, with their subsequent decay by light emission. In the analysis of the temperature dependence two activation energies emerge which are associated with the binding of excitons to erbium centers and with a transfer process from excited erbium ions back to erbium-bound excitons, respectively. The model provides good quantitative agreement with observations over the experimentally covered temperature range from 4 to nearly 200 K.

Introduction

The light emission in a wavelength range from about 1.54 to 1.60 μm of erbium in silicon has triggered considerable research activity in recent years. The eminent suitability of the erbium light as a carrier for long-distance signal transport via quartz fibers is a stimulation for such research from the application point of view. Important topics are the efficiency of the light emission and its quenching upon increase of the temperature, in particular to room temperature. As regards the fundamental science involved, the complex chain of processes by which excitation energy imparted to the host crystal is transferred to the final step of light emission by the $^4\text{I}_{13/2}$ to $^4\text{I}_{15/2}$ transition of 4f inner-shell electrons of erbium is a challenging topic in semiconductor physics.

In the present paper photoluminescence measurements are presented for both float-zoned, oxygen-lean, and Czochralski-grown, oxygen-rich, silicon samples doped with erbium by implantation. Measurements were also performed on a sample grown by a sublimation MBE method. The multiple component structure in the spectra confirms the existence of erbium-related centers of different symmetry, cubic and non-cubic, in these samples. The temperature dependencies were measured and are described by an excitation mechanism involving free and erbium-bound excitons as intermediate states. Results are analyzed on the basis of a model with particular consideration of the quantitative agreement achieved.

Experiment

The reported experiments were performed on samples with the following specifications.

1. Samples of float-zone (Fz), n-type phosphorus-doped, resistivity 0.8 $\Omega\cdot\text{cm}$, $\langle 100 \rangle$ -oriented silicon. The material was implanted with erbium ions at an energy of 1.1 MeV to a dose of 10^{13} cm^{-2} . Implantations were performed at 500 °C; no subsequent heat treatment has been applied. The samples are labeled Fz-Si:Er [1].
2. Samples of p-type Czochralski-grown (Cz) silicon with oxygen concentration of $2 \times 10^{18} \text{ cm}^{-3}$. The samples were implanted with erbium ions at the energy of 320 keV, to an erbium peak concentration of $5 \times 10^{17} \text{ cm}^{-3}$ and co-implanted with oxygen. A thermal anneal of 30 hours at 650 °C and 15 minutes at 900 °C was given to these samples, which are designated as Cz-Si:Er,O(1).
3. Samples of p-type Cz-Si material with the room-temperature resistivity of 1 to 10 $\Omega\cdot\text{cm}$. Wafers were implanted with erbium ions, with energy of 1.2 MeV, to a dose of 10^{13} cm^{-2} ; oxygen ions with the

energy 0.17 MeV were implanted to a dose of 10^{14} cm^{-2} . To optimize the luminescence output the samples received a post-implantation anneal for 0.5 hour at the temperature of 900 °C in a chlorine-containing atmosphere [2-3]. Such samples are labeled Cz-Si:Er,O(2).

4. A crystalline silicon layer, 2 μm thick, grown by a sublimation MBE method at 500 °C on top of a <100>-oriented p-type wafer [4]. After growth the sample was annealed at 700 °C for 30 minutes. The concentration of erbium, as measured by SIMS, was 10^{18} cm^{-3} . The sample is labeled MBE-Si:Er.

The luminescence was excited by the 514.5 nm line of an Ar⁺-ion laser. The laser power could be varied to correspond to an excitation power of 1 μW to 10 mW in the spot of about 1 mm diameter measured in front of the sample dewar. The emitted light was dispersed by a high-resolution 1.5 m grating monochromator and detected by a liquid-nitrogen cooled germanium photo-conductive detector. For the measurements of the temperature dependence of the PL intensity a cryostat with a variable temperature insert was used. The temperature of the samples was measured by a RhFe metallic resistor in a four-point-probe configuration to an accuracy of 0.1 K. Temperature control was achieved by PID regulation of the current through a heater wound on a copper block on which the samples were mounted. Experiments were performed in the 4.2 to 180 K temperature range.

Model

The model as will be discussed in this paper is illustrated by the scheme in Fig. 1. Energy imparted to the silicon crystal by the incident laser light is transferred to the erbium light emission on output via the intermediate processes of creation of free electrons and holes (concentration n), free excitons (concentration n_x), erbium-bound excitons (concentration n_{xb}) and erbium ions in excited state (concentration n_{Er}^*).

In the forward process of energy transfer leading to luminescence free electrons and holes are created by the incident light at the rate G . These free carriers can combine to form free excitons following a second-order process with the rate $\gamma_x n^2$. Trapping of the free excitons at free erbium sites will be proportional to both exciton and the available concentration of free erbium sites. This latter concentration is written as the total erbium concentration n_{Er} multiplied by the fraction of free sites $[(n_{Er} - n_{xb})/n_{Er}]$. Erbium-bound excitons can transfer their energy in an impurity Auger process to the 4f electrons of the erbium ion with a transfer time τ^* . At the same time a hot carrier accepting the excess energy E_A is formed. This process can only happen for erbium ions still in their ground state, i.e., to the fraction $[(n_{Er} - n_{Er}^*)/n_{Er}]$. At high excitation power these fractions given between the square brackets tend to zero and counteract further energy transfer. The exhaustion of the available erbium centers results in saturation of the luminescence. In the last step, the luminescence follows from decay of excited erbium ions n_{Er}^* with the time constant τ_d . The photoluminescence as measured in the experiment is proportional to this decay rate n_{Er}^*/τ_d . This decay, from an erbium $^4I_{13/2}$ excited to the $^4I_{15/2}$ ground state, is an internal atomic transition and is expected to have a temperature-independent time constant.

Reverse processes are indicated in Fig. 1 by the arrows pointing in the left direction. They include the dissociation of free excitons into free electrons and holes, the release of excitons from their erbium trapping sites and a back-transfer process in which an erbium bound exciton is recreated starting from an excited erbium ion. In such reverse processes the energy increases and they are therefore thermally activated by energies characteristic for the distinct processes, which are in the 5 to 150 meV range. Reverse processes, which reduce the luminescence output, are suppressed at the lowest temperatures. By the principle of detailed balance relations between the coefficients of forward and reverse processes can be established

Additional processes, not related to erbium luminescence but removing energy irreversibly from the chain, must be considered as well in the model. Two of such processes are indicated in Fig. 1 by arrows pointing downwards. They are the loss of free electrons and holes via recombination centers with the rate γn^2 , e.g., due to deep levels existing as the result of implantation damage and deciding on the lifetime of the carriers. The direct recombination of free excitons or via alternative centers also leads to loss of excitation energy.

The mathematical model based on the rate equations as introduced above has been discussed in some detail by Bresler *et al.* [5]. In a steady state the concentrations are described by the balance equations for free electrons, free excitons, bound excitons and excited erbium ions. Following the model these equations are, respectively,

$$G + fn_x = \gamma_x n^2 + \gamma n^2, \quad (1)$$

$$\gamma_x n^2 + cf_{xb} n_{xb} N_x = cn_x n_{Er} [(n_{Er} - n_{xb})/n_{Er}] + fn_x + n_x/\tau_x, \quad (2)$$

$$cn_x n_{Er} [(n_{Er} - n_{xb})/n_{Er}] + n_{Er}^* f_1/\tau^* = n_{xb} [(n_{Er} - n_{Er}^*)/n_{Er}]/\tau^* + cf_{xb} n_{xb} N_x, \quad (3)$$

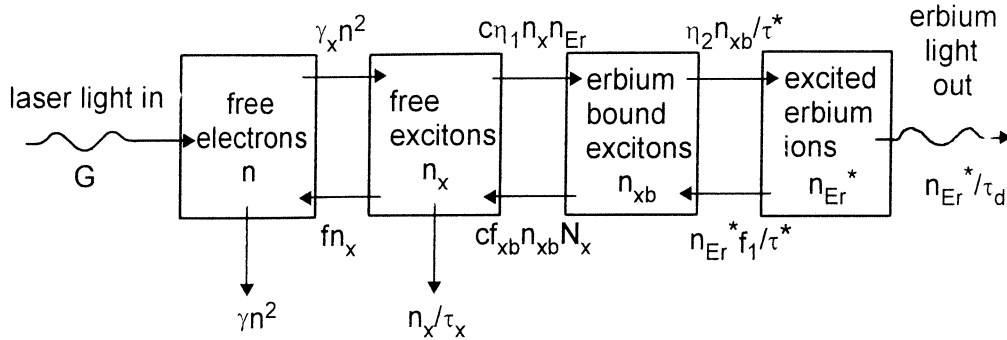


Fig. 1. Diagram indicating the physical processes by which energy is transferred between free electrons/holes (n), free excitons (n_x), erbium-bound excitons (n_{xb}) and erbium ions in excited state (n_{Er}^*) in the process of photo-excitation of the luminescence of erbium in silicon. An abbreviated notation $\eta_1 = (n_{Er} - n_{xb})/n_{Er}$ and $\eta_2 = (n_{Er} - n_{Er}^*)/n_{Er}$ is used.

$$\text{and} \quad n_{xb}[(n_{Er} - n_{Er}^*)/n_{Er}]/\tau^* = n_{Er}^*/\tau_d + n_{Er}^* f_1/\tau^*. \quad (4)$$

Generation terms are given in the left hand sides of these equations; the loss terms appear on the right. Relations between the coefficients of forward and reverse processes, based on detailed balancing of the separate steps, are

$$f = \gamma_x (N_c N_v / N_x) \exp(-E_x/kT), \quad (5)$$

$$f_{xb} = \exp(-E_{xb}/kT) N_x \exp(-E_{xb}/kT) / [N_x \exp(-E_{xb}/kT) + n_{Er}], \quad (6)$$

$$\text{and} \quad f_1 = \exp(-E_A/kT). \quad (7)$$

Characteristic energies involved in these process steps appear in the equations by E_x , the binding energy of electron and hole in an exciton, E_{xb} , the energy of binding of an exciton to a neutral erbium center and E_A , the energy dissipated in the creation of an excited erbium ion from the bound exciton situation. Densities of states in conduction, valence and exciton bands are found from the standard relations

$$N_c = 2(2\pi m_e kT/h^2)^{3/2}, \quad (8)$$

$$N_v = 2(2\pi m_h kT/h^2)^{3/2} \quad (9)$$

$$\text{and} \quad N_x = 2(2\pi m_x kT/h^2)^{3/2}, \quad (10)$$

with the appropriate effective masses. An exact solution of the balance equations is available in the form of a quadratic equation for n_{Er}^*/n_{Er}

$$a_0(n_{Er}^*/n_{Er})^2 - (b_0 + b_2 G)(n_{Er}^*/n_{Er}) + c_2 G = 0, \quad (11)$$

$$\text{with} \quad a_0 = +1 + c n_{Er} \tau_x [1 + (\tau^*/\tau_d) + f_1] + f \tau_x \gamma / (\gamma_x + \gamma), \quad (12)$$

$$b_0 = +1 + c n_{Er} \tau_x + f \tau_x \gamma / (\gamma_x + \gamma) + f_{xb} c N_x \tau^* [1 + f_1 (\tau_d/\tau^*)] [1 + f \tau_x \gamma / (\gamma_x + \gamma)], \quad (13)$$

$$b_2 = +c \tau_x \tau_d [1 + (\tau^*/\tau_d) + f_1] \gamma_x / (\gamma_x + \gamma) \quad (14)$$

$$\text{and} \quad c_2 = +c \tau_x \tau_d \gamma_x / (\gamma_x + \gamma). \quad (15)$$

Any temperature dependence in the model is included in the solution through the factors f , f_{xb} and f_1 .

Under conditions of high generation power G the approximate solution of equation (11) is given by $n_{Er}^*/n_{Er} = c_2/b_2$. With Eqs (14) and (15) one finds that the photoluminescence output saturates at

$$n_{Er}^*/n_{Er} = 1/[1 + (\tau^*/\tau_d) + f_1]. \quad (16)$$

This implies a very modest thermal effect. At high power the concentrations n_{xb} and n_{Er}^* are driven towards n_{Er} , nullifying the effect of the thermally induced reverse reactions. With numerical values $\tau^*/\tau_d \approx 10^{-3}$ and $E_A \approx 100$ meV the thermal quenching is predicted to be a few percent only at room

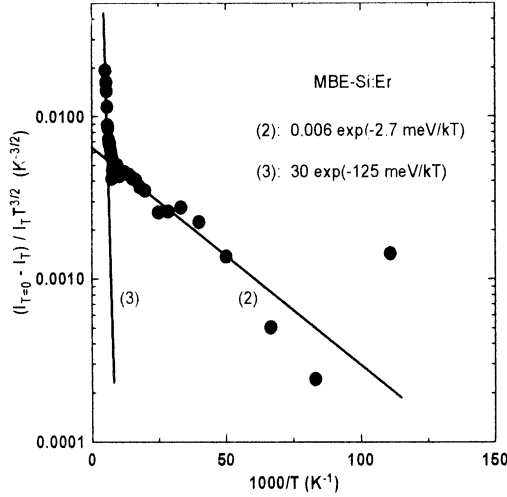


Fig. 2. Plot of $(I_{T=0} - I_T) / I_T T^{3/2}$ as a function of reciprocal temperature illustrating the analysis based on Eq. (24) for the MBE-Si:Er sample.

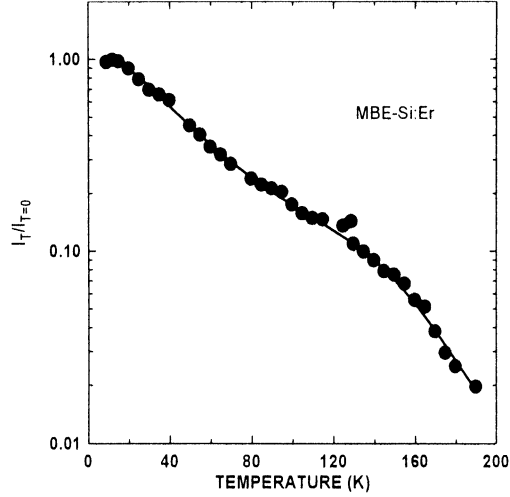


Fig. 3. Photoluminescence intensity as a function of sample temperature, normalized to the yield at low temperature, for the MBE-Si:Er sample. The solid line represents the fit with Eq. (22).

temperature. It thus appears that, at the expense of power efficiency, thermal quenching can be prevented. These conditions were not reached in our experiments.

The actual experiments were carried out at lower generation power. The applicable approximate solution $n_{Er}^*/n_{Er} = c_2 G/b_0$ represents the linear excitation regime. The model solution for n_{Er}^*/n_{Er} at the temperature T is

$$(n_{Er}^*/n_{Er})_T = [c\tau_x\tau_d\gamma_x/(\gamma_x + \gamma)]G/\{1 + cn_{Er}\tau_x + f\tau_x\gamma/(\gamma_x + \gamma) + f_{xb}cN_x\tau^*[1 + f_1(\tau_d/\tau^*)][1 + f\tau_x\gamma/(\gamma_x + \gamma)]\},$$

which for low temperature reduces to

$$(n_{Er}^*/n_{Er})_{T=0} = [c\tau_x\tau_d\gamma_x/(\gamma_x + \gamma)]G/(1 + cn_{Er}\tau_x). \quad (18)$$

The thermal quenching is given as the ratio

$$(n_{Er}^*)_T/(n_{Er}^*)_{T=0} = (1 + cn_{Er}\tau_x)/\{1 + cn_{Er}\tau_x + f\tau_x\gamma/(\gamma_x + \gamma) + f_{xb}cN_x\tau^*[1 + f_1(\tau_d/\tau^*)][1 + f\tau_x\gamma/(\gamma_x + \gamma)]\},$$

or

$$(n_{Er}^*)_T/(n_{Er}^*)_{T=0} = 1/\{1 + f\tau_x\gamma/(\gamma_x + \gamma)(1 + cn_{Er}\tau_x) + f_{xb}cN_x\tau^*[1 + f_1(\tau_d/\tau^*)][1 + f\tau_x\gamma/(\gamma_x + \gamma)]/(1 + cn_{Er}\tau_x)\}. \quad (20)$$

All temperature dependent parameters, f , f_{xb} and f_1 , are present in this result, but, as will be discussed below, they are not equally effective in the low- and high-temperature ranges.

Equilibrium between free electrons/holes and free excitons is controlled by the dimensionless factor $f\tau_x = \gamma_x\tau_x(N_eN_h/N_x)\exp(-E_x/kT)$. With numerical values $\gamma_x = 10^{12} \text{ cm}^3 \text{ s}^{-1}$ [6], and $\tau_x = 4 \times 10^{-6} \text{ s}$ [6], one estimates $f\tau_x \approx 4 \times 10^{-3} T^{3/2} \exp(-E_x/kT)$, which is smaller than 1 in the temperature range below 100 K, assuming binding energy $E_x \approx 15 \text{ meV}$. By introducing corresponding simplifications in Eq. (20) the activation energy E_x disappears from the model description and is therefore not determined in the experiment. In terms of physics this implies that the loss of free excitons by direct recombination, with the rate $1/\tau_x$, dominates over the loss by thermally induced dissociation, with the rate governed by f , in the temperature range considered.

Also the equilibrium between erbium-bound excitons and the erbium ions in excited state is not affected by thermal effects in the temperature range below around 100 K. From Eq. (20) one notes that the reverse reaction becomes of importance when $f_1(\tau_d/\tau^*)$ has risen towards unity. With the estimates

Table 1: Activation energies E_i and pre-exponential constants A_i derived from the temperature dependence of the photoluminescence of four different crystalline silicon samples. Following Eq. (24) fits were made to a sum of exponential functions $A_i \exp(-E_i/kT)$; $i = 1, \dots, 3$ as required for a satisfactory match. Several values of laser power were used for each sample.

Sample	Laser power (mW)	A_1 ($K^{-3/2}$)	E_1 (meV)	A_2 ($K^{-3/2}$)	E_2 (meV)	A_3 ($K^{-3/2}$)	E_3 (meV)
Fz-Si:Er	100	0.0024	1.1	0.037	14.5	2300	109
	150			0.04	12.2	32	92
	300			0.01	6.6	3.6	74
Cz-Si:Er,O(1)	100			0.21	13.6		
	150			0.09	9.9		
	200			0.07	10.8		
Cz-Si:Er,O(2)	50			0.35	12.9		
	100			0.46	15.6		
	150			0.21	11.4	575	120
MBE-Si:Er	100			0.006	3.6	370	123
	150			0.006	4.0	120	117
	200			0.006	2.7	30	125

$\tau_d/\tau^* \approx 10^3$ and $E_A \approx 100$ meV this will occur around $T = 150$ K. At lower temperatures this process of energy back transfer can be ignored.

The remaining temperature-dependent process is the equilibrium between free and erbium-bound excitons, represented in the equations by f_{xb} . This parameter expresses the balance of exciton capture between erbium, with concentration n_{Er} , and exciton density of states N_x . To judge this process it is assumed that the concentration of optically active erbium ions is much smaller than the total erbium concentration as was specified in the sample descriptions. The assumption that only around 1% of erbium is in the optically active state is also based on monitoring the emitted power in the erbium luminescence under conditions of their saturation and taking their radiative life time $\tau_d = 1$ ms. The density of states in the exciton band N_x will be in the range 2×10^{17} to $2 \times 10^{18} \text{ cm}^{-3}$ for temperatures from 20 to 100 K. With an estimate for E_{xb} between 10 and 15 meV the approximation $f_{xb} = \exp(-E_{xb}/kT)$ will be valid.

The above discussion leads to Eq. (20) in adapted form for low-temperature application:

$$(n_{Er}^*)_{T=0}/(n_{Er}^*)_{T=0} = 1/\{1 + [cN_x\tau^*/(1 + cn_{Er}\tau_x)]\exp(-E_{xb}/kT)\}. \quad (21)$$

To analyze experimental results obtained in the temperature range 100 to 200 K it is necessary to retain the factor $1 + f_1(\tau_d/\tau^*)$ of Eq. (20). In this way the whole temperature range is covered by

$$(n_{Er}^*)_{T=0}/(n_{Er}^*)_{T=0} = 1/\{1 + cN_x\tau^*\exp(-E_{xb}/kT)[1 + (\tau_d/\tau^*)\exp(-E_A/kT)]/(1 + cn_{Er}\tau_x)\}. \quad (22)$$

Again employing numerical estimates $c \approx 5 \times 10^{-10} \text{ cm}^3 \text{ s}^{-1}$, $n_{Er} \approx 5 \times 10^{15} \text{ cm}^{-3}$, $\tau_x \approx 4 \times 10^{-6} \text{ s}$, and calculating $cn_{Er}\tau_x \approx 10 \gg 1$, expression (22) further reduces to

$$(n_{Er}^*)_{T=0}/(n_{Er}^*)_{T=0} = 1/\{1 + (N_x\tau^*/n_{Er}\tau_x)\exp(-E_{xb}/kT)[1 + (\tau_d/\tau^*)\exp(-E_A/kT)]\}. \quad (23)$$

Noting that N_x contains the factor $T^{3/2}$ the temperature dependence can be made explicit by writing $N_x = (N_x/T^{3/2})T^{3/2}$. For the graphical presentation of experimental results Eq. (23) is used in the form

$$[(n_{Er}^*)_{T=0}/(n_{Er}^*)_{T=0} - 1]/T^{3/2} = [(N_x/T^{3/2})\tau^*/n_{Er}\tau_x]\exp(-E_{xb}/kT) + [(N_x/T^{3/2})\tau_d/n_{Er}\tau_x]\exp[-(E_A + E_{xb})/kT]. \quad (24)$$

The illustration of the analysis based on Eq. (24) for sample MBE-Si:Er is given in Fig. 2. Numerical

data obtained from the analysis are collected in Table 1 for all four samples and for a few levels of excitation power. Pre-exponential factors and energies in the table are identified with formula (24) by $A_2 \leftrightarrow (N_x/T^{3/2})\tau^*/n_{Er}\tau_x$, $A_3 \leftrightarrow (N_x/T^{3/2})\tau_d/n_{Er}\tau_x$, $E_2 \leftrightarrow E_{xb}$ and $E_3 \leftrightarrow E_{xb} + E_A$. With the parameters $N_x/T^{3/2} \approx 2 \times 10^{15} \text{ cm}^{-3} \text{ K}^{-3/2}$, $n_{Er} \approx 5 \times 10^{15} \text{ cm}^{-3}$ and $\tau^* \approx \tau_x$ the model predictions for the temperature-constant pre-exponential factors are $A_2 \leq 1 \text{ K}^{-3/2}$ and $A_3 = (\tau_d/\tau^*)A_2 \leq 10^3 \text{ K}^{-3/2}$. Taking into account the difficulty of precise determination of pre-exponential factors the experimental findings confirm the model. The smaller values for MBE-Si:Er may be related to the much larger erbium concentration in this sample. The data also tend to support the model prediction that for higher excitation power the temperature dependence becomes weaker. A dependence of activation energies on excitation power is not accounted for within the model. In the case of the Fz-Si:Er samples a third term with a small activation energy around 1 meV was helpful to improve the fit at the lowest temperatures. The origin of this term is not clear. Values for E_{xb} are found to be different for the four kinds of sample, suggestive for exciton binding to erbium-related centers with a different structure. Only one energy in the range 5-15 meV is required for the analyses. The absence of an $E_{xb} + E_x$ activation energy in the range 20 to 30 meV including an exciton dissociation energy is confirmed by this result. Fig. 3 demonstrates the quality of the fit; a good agreement may be concluded.

Conclusion

The temperature dependence of the photoluminescence intensity of erbium-doped silicon in the 1.54 μm spectrum has been measured. For the analysis a model was used in which the incident light energy is transferred via the intermediate stages of free electrons and holes, free excitons, and erbium-bound excitons to the intra-4f-shell excited erbium ions. The thermal dependence is governed by the binding energy of excitons to erbium centers in the temperature range below 100 K. The energy of binding electrons and holes together in an exciton does not have an effect on the temperature dependence and is hence not measured. At higher temperatures, above around 100 K, an activation energy near 100 meV becomes more prominent. This energy is associated with the transfer of energy from an excited erbium ion back to an erbium-bound exciton. Quite similar parameters are obtained for the erbium implanted samples; for the MBE grown sample with its higher erbium concentration smaller energy E_{xb} and smaller pre-factors are found. The optically active erbium ions appear to be a small fraction only, of order 1%, of the total erbium content. Enhancement of this fraction by improved technology will lead to substantially enlarged luminescence intensity.

Acknowledgments

The authors are grateful to F.P. Widdershoven, Philips Research, Eindhoven, The Netherlands, to L.C. Kimerling and J. Michel, MIT, Cambridge, USA and to N.A. Sobolev, A.F. Ioffe Physico-Technical Institute, St Petersburg, Russia for providing the erbium implanted samples, as well as to V.P. Kuznetsov, Institute for Physics of Microstructures, Nizhny Novgorod, Russia, who grew the MBE sample for the reported experiments.

References

- [1] F.P. Widdershoven, Doctor thesis, University of Twente, The Netherlands, 1991.
- [2] N.A. Sobolev, Semiconductors 29 (1995) p. 595 [translation from Fiz. Tekh. Poluprovodn. 29 (1995) p. 1153].
- [3] N.A. Sobolev, O.V. Alexandrov, V.V. Emtsev, M.I. Makoviicnuk, A.V. Merkulov, E.O. Parshin, D.S. Poloskin and E.I. Shek, Solid State Phenomena 47-48 (1996) p. 299.
- [4] M. Stepikhova, A. Andreev, B. Andreev, Z. Krasil'nik, V. Shmagin, V. Kuznetsov, R. Rubtsova, W. Jantsch, H. Ellmer, L. Palmethofer, H. Preier, Yu. Karpov, K. Piplits and H. Hutter, Acta Phys. Pol. A 94 (1998) p. 549.
- [5] M.S. Bresler, O.B. Gusev, B.P. Zakharchenya and I.N. Yassievich, Phys. Solid State 38 (1996) p. 813 [translation from Fiz. Tverd. Tela 38 (1996) p. 1474].
- [6] J. Palm, F. Gan, B. Zheng, J. Michel and L.C. Kimerling, Phys. Rev. B 54 (1996) p. 17603.